www.czasopisma.pan.pl PAN www.journals.pan.pl

ARCHIVES of FOUNDRY ENGINEERING

DE GRUYTER OPEN

ISSN (2299-2944)
Volume 17
Issue 4/2017

DOI: 10.1515/afe-2017-0154

Published quarterly as the organ of the Foundry Commission of the Polish Academy of Sciences

179 – 184

Microstructure and Mechanical Behavior of Mg-0.5Si-xSn Alloys

Xuesong Fu [a], Yan Yang [a, b] *, QuanYang Ma [a], Xiaodong Peng [a, b], Tiancai Xu [a]
[a] School of Materials Science and Engineering, Chongqing University, Chongqing 400044, China
[b] National Engineering Research Center for Magnesium Alloys, Chongqing University, Chongqing 400044, China
*Corresponding author. E-mail address: yanyang@cqu.edu.cn

Received 27.07.2017; accepted in revised form 29.09.2017

Abstract

Mg-0.5Si-xSn (x=0.95, 2.9, 5.02wt.%) alloys were cast and extruded at 593K (320 °C) with an extrusion ratio of 25. The microstructure and mechanical properties of as-cast and extruded test alloys were investigated by OM, SEM, XRD and tensile tests. The experimental results indicate that the microstructure of the Mg-0.5Si-xSn alloys consists of primary α-Mg dendrites and an interdendritic eutectic containing α-Mg, Mg_2Si and Mg_2Sn. There is no coarse primary Mg_2Si phase in the test alloys due to low Si content. With the increase in the Sn content, the Mg_2Si phase was refined. The shape of Mg_2Si phase was changed from branch to short bar, and the size of them were reduced. The ultimate tensile strength and yield strength of Mg-0.52Si-2.9Sn alloy at the temperature of 473K (200 °C) reach 133MPa and 112MPa respectively. Refined eutectic Mg_2Si phase and dispersed Mg_2Sn phase with good elevated temperature stability are beneficial to improve the elevated temperature performance of the alloys. However, with the excess addition of Sn, large block-like Mg_2Sn appears around the grain boundary leading to lower mechanical properties.

Keywords: Low-silicon magnesium alloy, Eutectic Mg_2Si, Microstructure, Mechanical behavior

1. Introduction

Magnesium alloys are regarded as one of the most significant resources in the 21th century, which has been extensively used in many fields such as automobiles, aerospace, and computers, etc. [1] However, their low strength at room temperature and elevated temperature restricts their wide applications. Many researchers have reported that various rare-earth elements and alkali element, for example, Y, Ca, Gd and Sc, can be mainly used by adding as alloying elements to improve the mechanical properties of magnesium alloys [2]. Usually, with the addition of these alloying elements as mentioned above, intermetallic phases with good elevated temperature stability are formed. The intermetallic phases can hinder the dislocation movements. Thus, the mechanical behavior of alloys can be improved not only at room temperatures but also at elevated temperatures [3]

However, applications of Mg-RE alloys with good elevated mechanical properties are limited because of the relatively high price. Also, adding RE elements into magnesium has the negative influence on low density for magnesium alloys. Thus, in this research, Si was identified as the adding alloying element to improve the elevated temperature mechanical behavior of magnesium alloys.

It has been reported that with the addition of Si into magnesium alloys, Mg_2Si phase with a melting point of 1085°C and hardness of 460 HV can be formed, which can improve the mechanical properties [4]. However, the morphology of Mg_2Si plays a critical role in improving the mechanical properties. Fine Mg_2Si particles contribute to the improvement in the mechanical behavior of the alloys. On the other hand, alloys with coarse Mg_2Si particles exhibit worse mechanical properties [5,6]. In general, the material matrix would be fragmented seriously by large primary Mg_2Si and dendritic eutectic Mg_2Si.

With the addition of Sn into magnesium alloys, Mg_2Sn with a high melting point is formed. Granular Mg_2Sn phase leads to dispersion enhancement to improve the materials' strength under room temperature and elevated temperature [7]. Furthermore, the addition of Sn can refine the Mg_2Si phase. Thus, it is possible to develop "RE-free" magnesium alloys with low density and good strength by adding Si and Sn into magnesium alloys [8]. However, review of the published literature shows that there is little information on the microstructure and mechanical behavior of Mg-Si-Sn ternary alloys. Thus, Mg-0.5Si-xSn alloys were prepared and investigated in the present study.

2. Experimental procedures

The raw materials used in the experiments were commercial pure magnesium (99.9 wt.%), pure tin (99.9 wt.%), and Mg-12Si master-alloy. Firstly, pure magnesium and Mg-12Si master alloys were loaded in a graphite crucible. The nominal composition of the alloys are listed in Table 1. Before the materials were heated, the furnace was filled with SF_6/CO_2 gas mixtures. Subsequently, the temperature of the resistance furnace was set to 993 K (720°C) to melt the materials. After the materials were melted, the temperature was decreased to 953 K (680°C) and tin was added into the melt. The alloy melt was maintained for 20min at 953 K (680°C). Finally, molten metal was poured into a casting metal mold (90 mm in diameter and 300 mm in height) to form as-cast specimens. Table 1 shows the true chemical composition of the experimental alloys.

Table 1.
Chemical composition of the experimental alloys (wt.%)

Alloy code	Nominal composition	Actual composition
1#	Mg-0.5Si-1Sn	Mg-0.46Si-0.95Sn
2#	Mg-0.5Si-3Sn	Mg-0.52Si-2.9Sn
3#	Mg-0.5Si-5Sn	Mg-0.48Si-5.02Sn

Then the specimens were homogenized at 533 K (260°C)×2 h for the forthcoming deformation process. During the deformation process, the ingots were extruded from Φ80 mm to Φ16 mm at 593 K (320°C) (extruding ratio is 25:1). The microstructure and phase composition of test alloys were investigated by OM, SEM, XRD, and EDS. According to the standard of ASTM E8M standard, standard tensile specimens with a gauge length of 30 mm and a gauge diameter of Φ6 mm were machined from the central part of the extrusion alloys. The model number of the testing machine is H25KL, which was made by Tinisolsen company. The gauge axes are parallel to the extrusion direction. Tensile tests of extruded Mg-0.5Si-xSn alloys were carried out at room temperature and 473 K (200°C) with a displacement speed of 2 mm/min. Three parallel tests were conducted to determine the reported strength and elongation.

3. Result and Discussion

3.1. Microstructure of Mg-0.5Si-xSn alloys

Fig. 1 shows the XRD pattern of Mg-0.5Si-xSn (x=0.95, 2.9, 5.02 wt.%) alloys. The results show that the alloy consists of α-Mg phase, Mg_2Sn intermetallic compounds, and Mg_2Si intermetallic compounds. With the increase in the Sn content from 0.95 wt.% to 5.02 wt.%, the peak intensity of Mg_2Sn increases modestly, which indicates the increase in the content of Mg_2Sn phase.

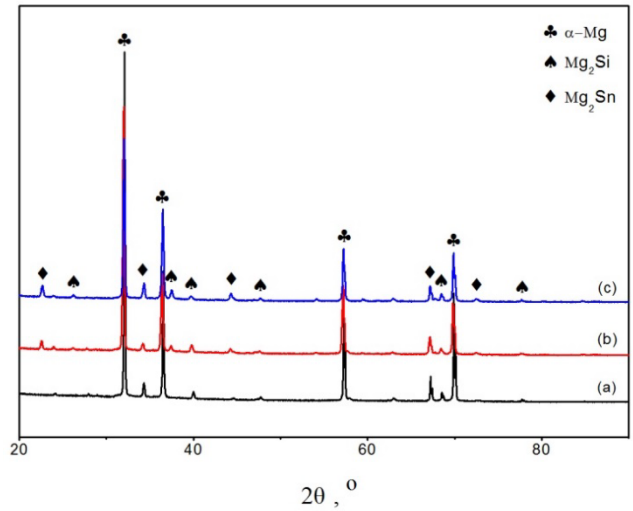

Fig. 1. XRD pattern of Mg-0.5Si-xSn alloys: (a) Mg-0.46Si-0.95Sn (b) Mg-0.52Si-2.9Sn (c) Mg-0.48Si-5.02Sn

The optical micrographs of the as-cast Mg-0.5Si-xSn alloys are shown in Fig. 2. The α phase (white) and dendritic phase (gray) distribute evenly in all the three alloys. The bright areas show a coarse bulk form of which the average phase size is approximately 80 μm in diameter. The dark areas mainly show a dendritic compound in which the average phase size is finer than bright areas. It is observed that the net-like phase is separated by boundaries of different phases and fills in the region between the bright phase. With the addition of Sn, the size of net-like phases are reduced from approximately 33 μm to 8 μm in diameter as shown in Fig. 2 (a) and (c). The net-like phase is refined efficiently, but the refinement of flake-like phase is not as efficient as that in net-like phase. The specimens are studied by SEM and EDS to confirm the compounds and microstructure in alloys.

The SEM images of as-cast Mg-0.5Si-xSn alloys are shown in Fig. 3, and the results of EDS are summarized in Table 2. Mg_2Si presented as two forms which are block-like primary grains in the α-Mg and branched-like eutectic grains around the boundary of α-Mg [9]. The block-like Mg_2Si couldn't be found in the α-Mg as shown in Fig. 3, so it indicates that low content of Si can avoid forming the primary Mg_2Si phase. The dark areas in SEM images correspond to the α-Mg phase in Fig. 2, and the EDS result

reveals that coarse net-like phase (compounds) in Fig. 2 enriches the elements of Mg and Si. It indicates that the net-like phase is Mg_2Si according to the EDS analysis. Some particles are found inside the α-Mg, and the enriched elements are Mg and Sn. Even the atomic ratio of Mg to Sn is about 2:1 as shown in Table 2. These tiny particles can be identified as Mg_2Sn. When the Sn content reaches 5 wt.%, the distribution of the Mg_2Sn compounds which appear along the grain boundaries is continuous in the as-cast alloys in Fig. 3 (c). Besides, coarse fishbone-like Mg_2Si is observed in the Fig. 3 (a). With the increase in the Sn, the size of fishbone-like Mg_2Si phases decrease continuously, and the morphology of Mg_2Si is changed from coarse fishbone-like phase to small bar-like phase. It is confirmed that the Mg_2Si phase can be refined by adding Sn.

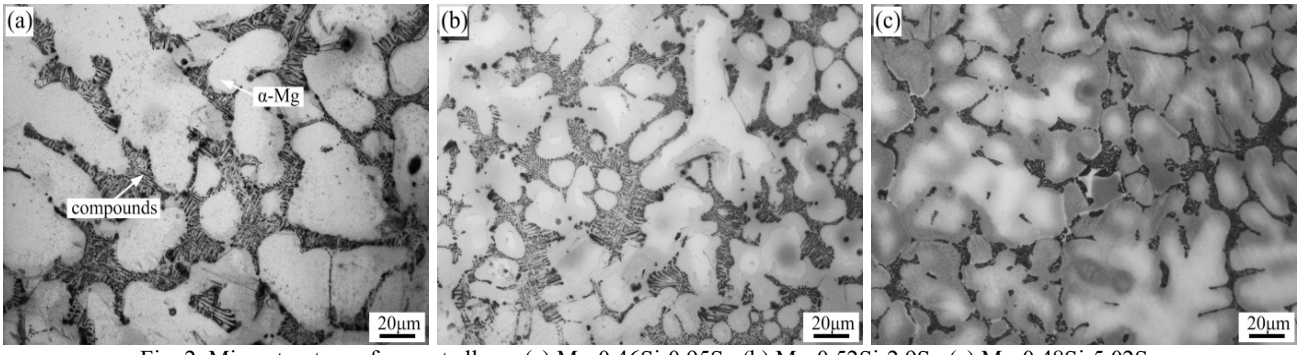

Fig. 2. Microstructure of as-cast alloys: (a) Mg-0.46Si-0.95Sn (b) Mg-0.52Si-2.9Sn (c) Mg-0.48Si-5.02Sn

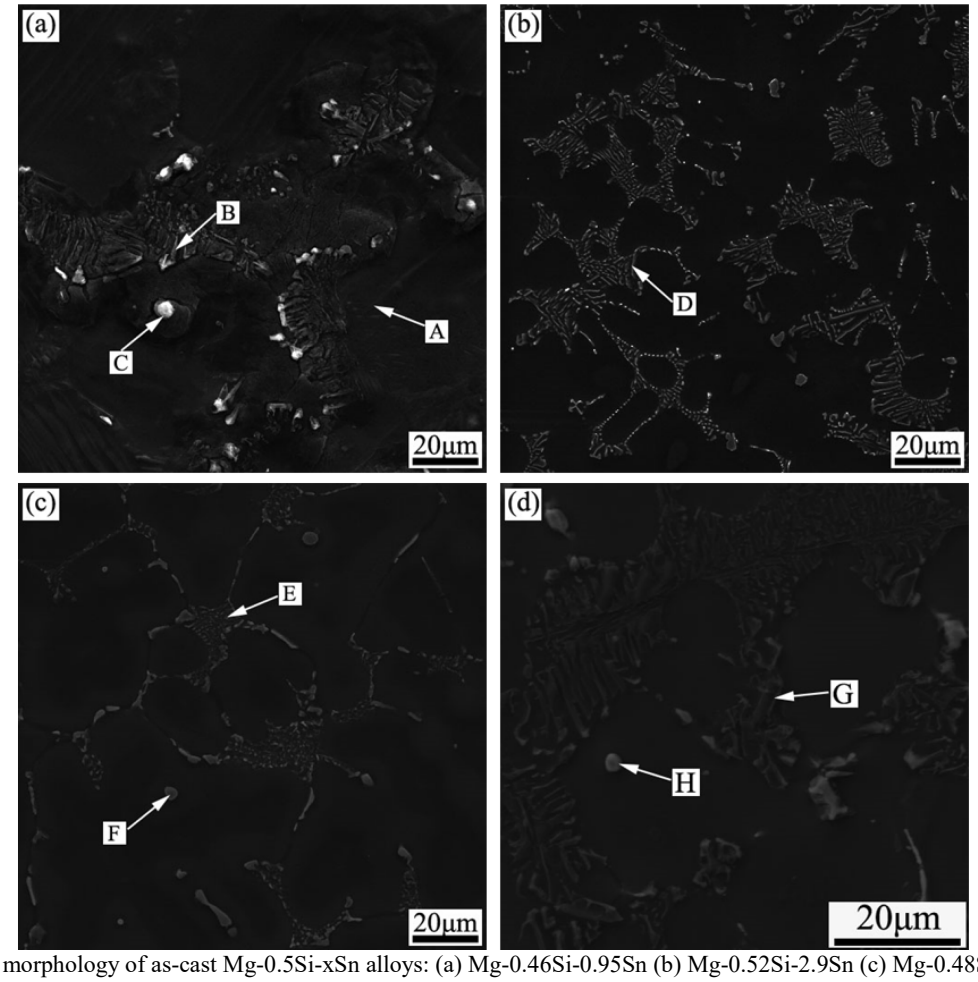

Fig. 3. SEM morphology of as-cast Mg-0.5Si-xSn alloys: (a) Mg-0.46Si-0.95Sn (b) Mg-0.52Si-2.9Sn (c) Mg-0.48Si-5.02Sn (d) Mg-0.52Si-2.9Sn at high magnification

Table 2.
EDS results at different positions in Fig. 3

Position	Molar fraction/%		
	Mg	Si	Sn
A	100	0	0
B	68.32	29.62	2.06
C	86.00	6.60	11.41
D	74.44	22.98	2.58
E	80.98	17.79	1.24
F	88.54	0	11.46
G	69.13	26.84	4.03
H	64.65	2.49	32.85

The microstructure of extruded Mg-0.5Si-xSn alloys is vertical to the extrusion direction as shown in Fig. 4. After the extrusion process, the α-Mg phase and the compounds are greatly refined, and the α-Mg phase is twisted as a result of severe deformation. Compared with microstructure shown in Fig. 3, the phases of extruded alloys are finer than that of as-cast alloys. The EDS point analysis of as-extruded alloys is displayed in Table 3. After the process of extrusion, the coarse fishbone-like Mg_2Si phase is broken, which is located on the boundary of α-Mg mixed some Mg_2Sn particles. The small particle phase (labeled as D), where both Mg and Si elements are detected is deduced to be Mg_2Si. It indicates that the dendritic Mg_2Si is crushed and distributes uniformly in the matrix. The large precipitated phase (labeled as F), where both Mg and Sn elements are detected is deduced to be Mg_2Sn.The details of the distraction of Si and Sn are studied in subsequent images.

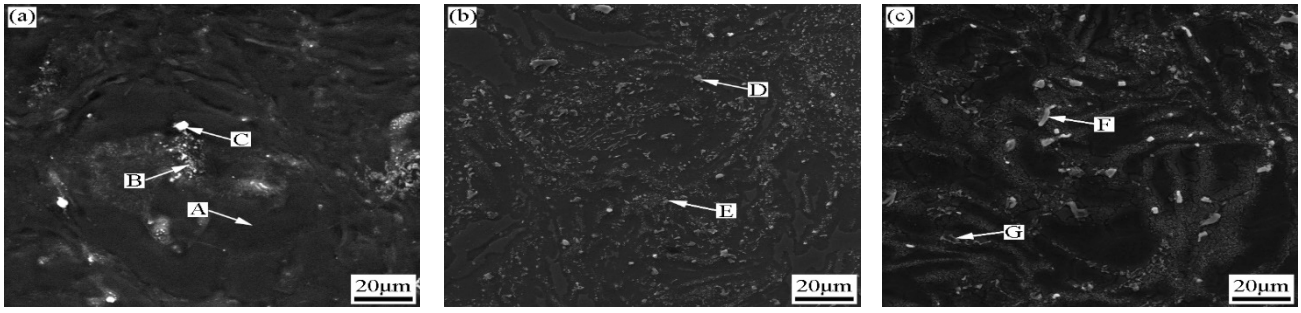

Fig. 4. Microstructure of as-extruded Φ16 mm Mg-0.5Si-xSn alloys：(a) Mg-0.46Si-0.95Sn (b) Mg-0.52Si-2.9Sn (c) Mg-0.48Si-5.02Sn

Table 3.
EDS results at different positions in Fig. 4

Position	Molar fraction/%		
	Mg	Si	Sn
A	100	0	0
B	92.46	5.91	1.63
C	72.19	22.15	5.66
D	76.61	20.74	2.64
E	98.45	0	1.55
F	71.31	0	28.69
G	78.43	18.59	2.99

3.2. Mechanical behavior of extruded Mg-0.5Si-xSn alloys

Tensile tests of extruded Mg-0.5Si-xSn alloys were performed along the extrusion direction with a displacement speed of 2 mm/min. The initial strain rate is $1.1\times10^{-3}s^{-1}$. The engineering stress-strain curves were recorded for each specimen as shown in Fig. 5. The tensile properties of extruded alloys with different Sn content at room temperature are presented in Table 4. The yield strength, ultimate tensile strength, and elongation of Mg-0.46Si-0.95Sn alloy are 158 MPa, 232 MPa, and 10% respectively. With the increase in the Sn content, the strength and ductility of the alloys slightly decrease. The ultimate tensile strength of Mg-0.52Si-2.9Sn alloy reached 229 MPa, and that of Mg-0.48Si-5.02Sn alloy reached 216 MPa. Elongation of Mg-0.46Si-0.95Sn alloy (10%) is higher than that of Mg-0.52Si-2.9Sn alloy (4%) and Mg-0.48Si-5.02Sn alloy (2%) at room temperature.

Fig.6 displays engineering tensile stress-strain curves of extruded Mg-0.5Si-xSn alloys at 473 K (200°C). The tensile properties of the extruded samples are listed in Table 5.With increasing Sn addition from 0.95 to 2.9 and 5.02 wt.%, elongation was decreased slightly from 38% to 30% and 36%. However, the ultimate tensile strength was improved remarkably from 106MPa to 133MPa and 118MPa at 473 K (200°C) due to the effective providing barriers to gliding dislocation during deformation. It exhibits that the yield and ultimate tensile strength of the extruded Mg-0.5Si-2.9Sn alloy (112MPa and 133MPa) are higher than those of the extruded Mg-0.5Si-0.95Sn alloy (88MPa and 106MPa). This indicates that the strength properties of the Mg-0.5Si-0.95Sn alloy are greatly improved by adding the element of Sn. However, the strength decreases when the content of Sn from 3 wt.% to 5 wt.%. Mg_2Sn particles play an important role in the second phase in improving the strength of materials [10,11].

Mg_2Sn as tiny particles distribute evenly in the phase boundary and matrix when the content of Sn is low. Particles restrict grain boundaries sliding, moving and rotating, which can block the dislocation obviously and improve strength consequently.[12,13] However, the strength decreases when the content of Sn arrived at 5 wt.% since continuous Mg_2Sn phase appears and splits the matrix. Plastic phases were separated by brittle phases, which restrict plasticity. Correspondingly, strength and plasticity can decrease owing to the cracks appeared after slight deformation. The present results show that the extruded alloys with 3 wt.% Sn addition resulted in better mechanical properties than those with Sn containing alloy.

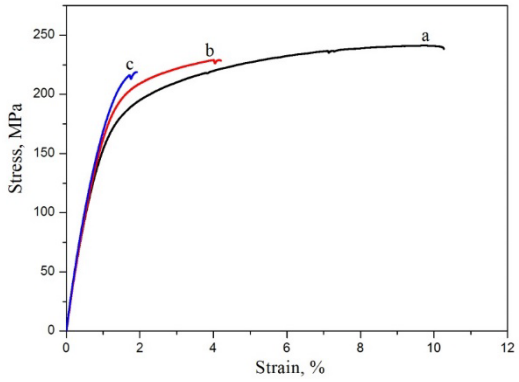

Fig. 5. The engineering tensile stress-strain curves of extruded alloys at room temperature: (a) Mg-0.46Si-0.95Sn (b) Mg-0.52Si-2.9Sn (c) Mg-0.48Si-5.02Sn

Table 4.
Mechanical properties of extruded Mg-0.5Si-xSn alloys at room temperature

Specimens	Yield strength /MPa	Ultimate tensile strength /MPa	Total strain /%
Mg-0.46Si-0.95Sn	158	232	10
Mg-0.52Si-2.9Sn	163	229	4
Mg-0.48Si-5.02Sn	157	216	2

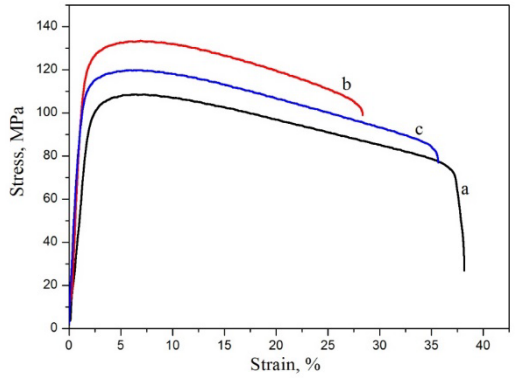

Fig. 6. The engineering tensile stress-strain curves of as-extruded alloys at 437 K (200°C): (a)Mg-0.46Si-0.95Sn (b) Mg-0.52Si-2.9Sn (c) Mg-0.48Si-5.02Sn

Table 5.
Mechanical properties of extruded Mg-0.5Si-xSn alloys at 473 K (200°C)

Specimens	Yield strength/ MPa	Ultimate tensile strength/ MPa	Total strain /%
Mg-0.46Si-0.95Sn	88	106	38
Mg-0.52Si-2.9Sn	112	133	30
Mg-0.48Si-5.02Sn	94	118	36

3.3. Fracture analysis

After the tensile tests, the fracture surfaces of the specimens were examined using SEM technique. Fracture morphology of the extruded Mg-0.5Si-xSn alloys at room temperature and elevated temperature are shown in Fig. 7. As displayed in Fig. 7 (a), (c) and (e), cleavage planes and a few dimples are found in these fracture surfaces of the as-extruded Mg-0.5Si-xSn alloys. It indicates that the fracture mechanism is mainly attributed to brittle fracture and a little ductility at room temperature. In addition, the fracture surfaces, which are tensed at 473 K (200°C), are shown in Fig. 7 (b), (d) and (f). The fracture microstructures are made up of deep dimples, typical characters of ductile fracture, which is consistent with the good ductility at 473 K (200°C). When the content of Sn reached 1 wt.% (shown in Fig. 7 (b)), more dimples and few compounds appear on fracture surfaces, whereas many intermetallic compounds can be observed in the fracture surface when the content of Sn reached 5 wt.% (shown in Fig. 7 (e) and (f)).

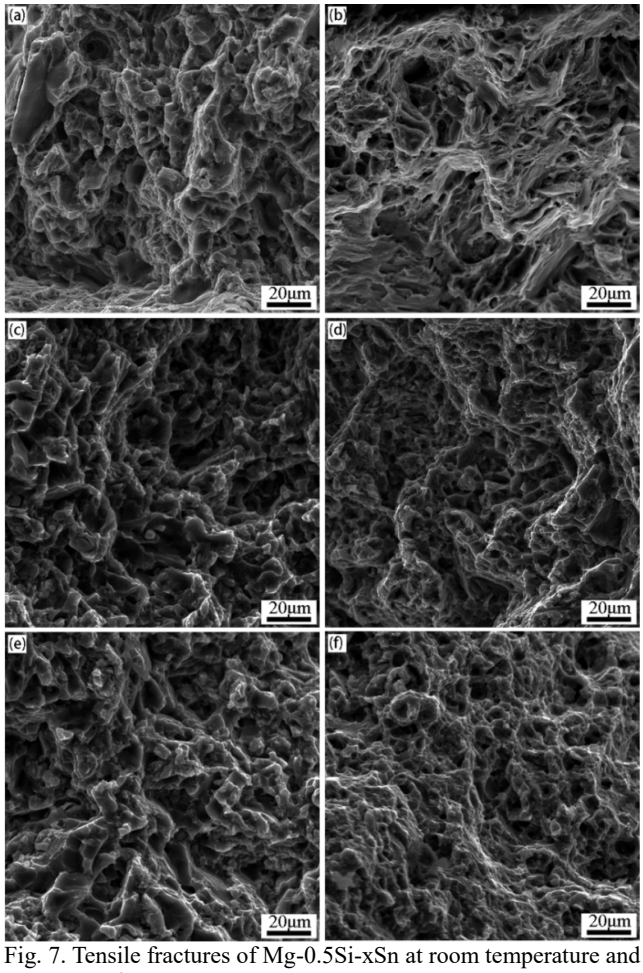

Fig. 7. Tensile fractures of Mg-0.5Si-xSn at room temperature and 473 K (200°C): Mg-0.5Si-0.95Sn at (a) room temperature and (b) at 473 K (200°C); Mg-0.5Si-2.9Sn at (c) room temperature and (d) at 473 K (200°C); Mg-0.5Si-5.02Sn at (e) room temperature and (f) at 473 K (200°C)

4. Conclusion

In this study, effects of Sn addition on microstructure and mechanical properties of extruded alloys at room temperature and elevated temperature have been investigated.

1. Mg-0.5Si-xSn alloys contain α-Mg (hcp) phase, eutectic Mg_2Si compounds and Mg_2Sn compounds. With the addition of Sn, the coarse net-like Mg_2Si compounds can be refined continuously and form particles of Mg_2Sn in matrix materials. However, the Mg_2Sn phase becomes continuous bar-like compounds when the content of Sn reached 5 wt.%.
2. With increasing Sn addition from 1 wt.% to 5 wt.%, the ultimate tensile strength was decreased from 232MPa to 216MPa at room temperature. However, at 473 K (200°C), the extruded Mg-0.5Si-xSn specimens first increase and then decrease. Mg-0.5Si-2.9Sn exhibits 112 MPa of yield strength and 133 MPa of ultimate tensile strength, which is higher than those of the extruded Mg-0.5Si-0.95Sn and Mg-0.5Si-5.02Sn specimens.
3. The fracture surfaces of extruded Mg-0.5Si-xSn alloys indicate brittle fracture at room temperature. However, samples contain evenly sized dimples at 473 K (200°C), indicating ductile fracture.

Acknowledgements

The authors would like to acknowledge financial support by the National Natural Science Foundation of China (Project No. 51601024), the National Natural Science Foundation of China (Grant Nos. 51701026), the National Key Research and Development Program of China plan (Project No. 2016YFB0700403), the Chongqing Research Program of Basic Research and Frontier Technology (Project No. cstc2016jcyjA0418) and the Fundamental Research Funds for the Central Universities (Project No. 106112017CDJXY130001).

References

[1] Zhang, X., Deng, K.K. & Li, W.J. (2015). Microstructure and mechanical properties of Mg-Al-Ca alloy influenced by SiCp size. *Materials Science & Engineering A*. 647, 15-27.

[2] Wang, X., Guo, M. & Zhang. J. (2016). Effect of Zn addition on the microstructure, texture evolution and mechanical properties of Al-Mg-Si-Cu alloys. *Materials Science & Engineering A*. 677, 522-533.

[3] Chi, H., Sun, H. & Zhang, Q. (2014). Advanced thermo electrics governed by a single parabolic band: Mg-Si-Sn, a canonical example. *Physical Chemistry Chemical Physics*. 16(15), 6893-6897.

[4] Oñorbe, E., Garcés, G. & Dobes, F. (2013). High-Temperature Mechanical Behavior of Extruded Mg-Y-Zn Alloy Containing LPSO Phases. *Metallurgical & Materials Transactions A*. 44(6), 2869-2883.

[5] Homma, T., Kunito, N. & Kamado, S. (2009). Fabrication of extraordinary high-strength magnesium alloy by hot extrusion. *Scripta Materialia*. 61(6), 644-647.

[6] Zhai, W., Lu, H. & Wu, C. (2013). Stimulatory effects of the ionic products from Ca-Mg-Si bioceramics on both osteogenesis and angiogenesis in vitro. *Acta Biomaterialia*. 9(8), 8004-8014.

[7] Yu, X., Jiang, B. & Yang, H. (2015). High temperature oxidation behavior of Mg-Y-Sn, Mg-Y, Mg-Sn alloys and its effect on corrosion property. *Applied Surface Science*. 353, 1013-1022.

[8] Nam, K.Y., Song, D.H. & Lee, C.W. (2006). Modification of Mg_2Si Morphology in As-Cast Mg-Al-Si Alloys with Strontium and Antimony. *Materials Science Forum*. 238-241.

[9] Liu, K., Du, W. & Li, S. (2016). The effect of heat treatment on microstructure of the melt-spun Mg–7Y–4Gd–5Zn–0.4Zr alloy. *Journal of Magnesium & Alloys*. 4(2), 99-103.

[10] Nadella, R., Sahu, S.N. & Gokhale, A.A. (2013). Foaming characteristics of Al–Si–Mg (LM25) alloy prepared by liquid metal processing. *Materials Science & Technology*. 26(8), 908-913.

[11] Dharmendra, C. & Rao, K.P. (2012). Hot working mechanisms and texture development in Mg-3Sn-2Ca-0.4Al alloy. *Materials Chemistry & Physics*. 136(2-3), 1081-1091.

[12] Jiang, G., He, J. & Zhu, T. (2014). High performance Mg_2(Si, Sn) solid solutions. *Advanced Functional Materials*. 24(24), 3776-3781.

[13] Zhao, C., Pan, F. & Zhao, S. (2015). Microstructure, corrosion behavior and cytotoxicity of biodegradable Mg-Sn implant alloys prepared by sub-rapid solidification. *Materials Science & Engineering C Materials for Biological Applications*. 54, 245-251.